ORIGINAL ARTICLE

Spectroscopic analysis of dissolved organic matter in industrial sludge composting process

Dezhi Tai[1] · Hua Zhang[1] · Asfandyar Shahab[1] · Jixing Yu[1] · Ankit Garg[2]

Abstract

Dissolved organic matter (DOM) not only reflects the biochemical transformation of organic matter during the composting process, but also evaluates the humification degree of composting. However, most research focuses on laboratory composting of DOM. In this study, the stability and maturity of DOM in large-scale industrial sludge compost were studied by basic physical, chemical parameters and spectral technology. The results showed that the initial temperature of compost increased rapidly, the high temperature period was longer, and the pH value first increased and then stabilized. The increase in the UV–Vis characteristic values $SUVA_{280}$ and $SUVA_{254}$ and the decrease in E_{250}/E_{365} and S_R indicated an increased humus content. Fourier transform infrared spectroscopy (FTIR) analysis showed that easily degradable substances such as polysaccharides and carbohydrates were decomposed into humic substances. The absorption rate of $1645\ cm^{-1}/1103\ cm^{-1}$, $1645\ cm^{-1}/1400\ cm^{-1}$, and $1645\ cm^{-1}/2930\ cm^{-1}$ confirmed that humic substances increased with the decomposition of polysaccharide compounds and alcohols. Fluorescence excitation-emission matrix spectroscopy (EEM) combined with parallel factor analysis (PFA) showed a gradual decrease in the C3 fraction representing the protein, with decomposition and conversion to humic and xanthate fractions, which was also confirmed by the four-component model (Fmax), the fluorescence region integral (FRI), and the humification index (HIX). This study uses a variety of spectral techniques combined with basic physicochemical parameters to assess the humification of industrial sludge composting, which provides a reference for guiding large-scale composting.

Keywords Sewage sludge · Composting · Spectroscopy · PARAFAC · Dissolved organic matter

1 Introduction

In recent years, the production of municipal sewage sludge wastes has remarkably increased in China. Meanwhile, it threatens the ecological environment, living organisms, and human beings. Ministry of Housing and Construction of China estimated that urban sludge production was about 58 million tons in 2020, while it was 37 million tons in 2015, showing that the average annual sludge production increased more than 26% [1]. The most common nutrients in mud are nitrogen (N), phosphorus (P), and potassium (K). In addition, it also contains more than 50% of protein, polysaccharide, lipid, and other organic substances [2]. Therefore, it can be used as a fertilizer in soil [3, 4]. However, sewage sludge contains a large number of organic and chemical pollutants including pathogens, heavy metals, parasites, and other pollutants [5, 6], which can be toxic to soil and plants. If untreated sludge is directly applied to the soil, it leads toward soil pH change and fertility loss. For this reason, the harmless disposal of sludge as a resource has become an issue that needs to be addressed in modern society [2, 7].

Nowadays, the main treatment methods of sludge in the world are sanitary landfill, incineration, and composting [8, 9]. At present, the main method of sludge treatment in China is sludge landfill [8, 10]. Compared with other methods, sanitary landfills has the advantages of being simple, ease of operation, low cost, and strong adaptability, but the disadvantages of subsequent management and maintenance difficulties make the future of sanitary

✉ Hua Zhang
zhanghua@glut.edu.cn

✉ Asfandyar Shahab
2017022@glut.edu.cn

1 College of Environmental Science & Engineering, Guilin University of Technology, Guilin 541004, China

2 Department of Civil and Environmental Engineering, Shantou University, Shantou 515063, China

landfill doubtful [8]. Composting is an economically viable, environmentally friendly, and sustainable method of sludge treatment [6, 11], which can stabilize the organic matter in sludge, inactive the pathogen flora and reduce the content of organic pollutants, and N, P, and K can be retrieved from sludge [3, 7, 12]. If the sludge has a low C/N ratio, then it is highly water-soluble and has a small particle size, making it unsuitable for composting alone. Generally, it needs to be mixed with straw, rice bran, and other auxiliary materials for composting [13, 14].

Compost is a biological process in which microbes are mineralized and humified. The development and activity of microorganisms in the water-soluble stage bring a biochemical transformation of organic matter in the reactor, and the resulting DOM characteristics can directly reflect the majority of the transformation processes of organic matter [8, 15, 16]. DOM is an active component in composting organic matter, including small molecular substances (free amino acids and sugars) and macromolecular substances (proteins and humus) [17]. Therefore, the analysis of DOM can provide key information for the assessment of humification. In the composting process, DOM will complex heavy metals, causing some environmental pollution.

Spectroscopic techniques are widely used in the study of DOM methods for judging humification. Ultraviolet spectroscopy (UV–visible) can accurately and quickly evaluate compost humification. Parallel factor analysis and fluorescence spectroscopy can be used to identify the transformative changes and origins of DOM. FTIR can identify the changes of chemical groups in DOM and better explain the maturity of compost [18–22]. However, due to the complexity and dispersion of the molecular composition of DOM, a single spectroscopic technique can not accurately and comprehensively assess the humification of compost [21, 23]. The UV–visible and FTIR examination of date palm compost (DOM) presented the degradation of organic matter and hydrophilic compounds which suggest the biodegradation and mineralization of organic matter in different compost samples [24]. DOM analysis of sludge and kitchen waste compost shows the soluble microbial by-products such as tyrosine and tryptophan loss with the gradual appearance of humic acid-like substances based on fluorescence excitation-emission spectroscopy [9]. Abaker [25] uses UV–visible and fluorescence spectroscopy combined with mathematical processing for sludge and green waste co-composting analysis to screen parameters for evaluating the chemical stability of compost. FTIR analysis of co-composting sludge with olive processed waste showed microbial degradation of lipids and carbohydrates [5]. However, most of the research reports sludge composting under laboratory conditions, while limited studies focused on large-scale industrial sludge composting performed in composting plants.

Considering the present gap in literature, this study focused on large-scale industrial sludge composting, while the objective of this study was (1) preliminary determination of compost maturity by basic physicochemical parameters; (2) determination of humification degree at large-scale industrial sludge compost by changes in spectral characteristics of DOM by UV–visible, FTIR, and EEM-PARAFAC; (3) combined with correlation analysis, the relationship between compost maturity and spectral indicators and physical and chemical parameters was clarified, and parameters that could accurately evaluate the degree of compost humification were found. As a result of this study, a reference can be provided for large-scale industrial composting, and spectral indicators can be used to determine the degree of humification in the composting process.

2 Materials and methods

2.1 Composting process and sampling

Composting raw materials included sludge (which was the excess sludge produced by the sewage treatment plant in Guilin city of China during the urban sewage treatment process) and rice bran (obtained from a local agricultural and sideline product processing plant). Rice bran and sludge (1:4) were mixed together for aerobic composting. The treatment plant adopts static closed bin type fermentation for 2 bins (8 stacks per bin, each stack 43 m × 1 m × 1 m), with bottom aeration and controlled temperature at 55 ℃, up to 70 ℃. The fermentation for static bin was 20 days, while dynamic fermentation (post-ripening fermentation) maturation was 7–11 days. The whole composting cycle was 31 days. Three parallel compost samples (each about 0.5 kg) were collected at 0, 4, 8, 20, and 31 days. The samples were uniformly mixed from the top, middle, and bottom of the pile.

2.2 The extraction of dissolved organic matter

In order to extract DOM, compost samples were collected, and a specific procedure was employed. The extracted sample was freeze-dried with deionized water (1:10, dry weight) and shaken for 24 h at 25 ℃ in the dark using a reciprocating shaker at 200 rpm/min, and the suspension was centrifuged at 12,000 rpm for 20 min following filtration through a filter of 0.45 μm. The extracted DOM was freeze-dried and used for UV–visible, FTIR, and EEM-PARAFAC analysis. A Shimadzu L series TOC analyzer (Shimadzu, Japan) was used to measure the dissolved organic carbon content of DOM [16].

2.3 UV–visible spectroscopy

The UV absorbance of DOM ranging from 200 to 800 nm was recorded using a Shimadzu UV-1800 spectrophotometer, and deionized (DI) water was used as a reference. To characterize DOM, two mass parameters, such as $SUVA_{254}$ and $SUVA_{280}$, were decided ($SUVA_{254} = ABS_{254} \times 100/TOC$; $SUVA_{280} = ABS_{280} \times 100/TOC$); the absorbance ratio of 250 nm and 365 nm (E_{250}/E_{365}) was determined to describe the humification intensity [24]. S_R ($S_{275-295}/S_{350-400}$) ($S_{275-295}$: the slope of the absorption curve in the UV wavelength range of 275 to 295 nm; $S_{350-400}$: the slope of the absorption curve in the UV wavelength range of 350 to 400 nm) was calculated, and this value was negatively correlate with compost humification intensity [26].

2.4 Fourier transforms infrared spectroscopy

Nicolet Nexus FTIR spectrophotometer was employed for the investigation of functional group changes in the required sample and the spectra were recorded ranging from 4000 to 400 cm^{-1}. For this purpose, 1 mg of freeze-dried DOM with 300 mg of dried spectral grade KBr was used to obtain FTIR spectra. Changes in organic structure and aromaticity in DOM were assessed using peak intensity ratios of 1645 cm^{-1}/1103 cm^{-1}, 1645 cm^{-1}/1400 cm^{-1}, and 1645 cm^{-1}/2930 cm^{-1}.

2.5 Fluorescence spectroscopy

DOM extracted from samples of different composting times were subjected to fluorescence measurement by using F-7000 fluorescence photometer (F-7000; Hitachi, Japan) in scanning mode [27]. The slit width of the excitation spectrum was 10 nm, while emission spectrum was 1 nm, with a scanning speed of 1000 nm min^{-1}. The emission spectra ranging from 280 to 520 nm were obtained at excitation wavelength of 254 nm, and the excitation spectra in the range of 300–600 nm were obtained at the emission wavelength of 520 nm. Synchronization was achieved by using wavelengths between 200 and 500 nm for excitation and 250 and 550 nm for emission [28].

2.6 PARAFAC analysis

PARAFAC analysis of EEM spectral data was performed in MATLAB 2017a using the freely downloadable DOMFlour (www.models.life.ku.dk) toolbox, following [29] tutorials for processing EEM data to minimize scattered rays and other effects in the EEM landscape.

The EEM data of the control Milli-Q water sample were subtracted from each EEM in the DOM sample to remove the lower Raman scattering rays, followed by the removal of first- and second-order Rayleigh and Raman scattering according to the protocol of Bahram et al. PARAFAC models were calculated for 2 to 7 components, and the identified components were examined by visual determination, residual analysis and splitting analysis. In this study, the maximum fluorescence intensity (Fmax) (a.u) values were used to calculate the relative concentrations of the corresponding components [30]. EEM matrices with excitation wavelengths of 200–500 nm and emission wavelengths of 250–550 nm were used for PARAFAC modeling.

2.7 Statistical analysis

The data was statistically analyzed by using Origin 2018 and MATLAB 2017a with SPSS v18.0 software.

3 Results and discussion

3.1 Changes in pH, MC, and temperature during composting

The temperature is one of the most intuitive and important parameters when evaluating the humification process of compost, reflecting information such as the metabolic activity of microorganisms in the pile [24, 31]. The temperature of the pile was kept above 60 ℃ in the first 3 days of composting (Table 1) which was due to the abundant amount of nutrients decomposition in pile by microorganisms. The production and metabolic activities were vigorous which release a large amount of heat [32]. The fluctuation of temperature in composting process is caused by the sampling of pile turnover. The oxygen content in the turned pile increases, and the temperature rises after a short mixing period, as evidenced by the temperature on the 4th and 8th days. During the high-temperature period of composting, the thermophilic microorganisms in the pile will multiply and dominate, causing the organic matter in the pile to be further decomposed with continuous heat emission. During this period, parasites and pathogenic microorganisms in the compost are killed,

Table 1 Basic physicochemical parameters of DOM samples at different times of industrial composting

Composting duration (day)	pH	Moisture content (%)	Windrow temperature (℃)	Ambient temperature (℃)
0 d	8.45	60.1	66.3	9.5
4 d	9.32	56.5	56	15.2
8 d	9.19	53.4	57.3	20.2
20 d	7.30	49	18.2	13.8
31 d	7.14	46.1	15.6	13.8

reaching the hygienic target that the compost temperature is greater than 50 °C for more than 3 days [2, 5].

It is important to maintain sufficient water content in the pile to ensure microorganism growth and their metabolism and to provide the medium for biochemical reactions. High moisture content affects the voids in the stack and weakens the ventilation effect, which is not conducive to the normal decomposition of compost [33]. The moisture content of the pile was gradually decreased due to the evaporation of water from the pile as heat generated during the composting process, which leads to decrease in microbial decomposition rate (Table 1). It is worth noting that there is a small rebound in water content on 4th and 8th day of high-temperature period, which may be due to the hydrolysis of some organic substances during the composting.

Another important factor that affects the quality of compost is pH value of compost [2, 34]. In compost with proper pH, microorganisms can grow and multiply better, further break down organic material, and improve compost maturity [23]. At the initial stage of composting, the pH value of the compost showed an increasing trend which was due to the massive metabolic decomposition of proteins in the pile by microorganisms during the high-temperature period resulting in the accumulation of NH_4^+-H, which leads toward rise in pH (Table 1) [2]. When the compost enters the cooling decomposition stage, as the easily decomposed organic material is consumed, the microorganisms begin to decompose the more difficult to decompose organic material. The biodegradation of refractory organic matter produces low molecular weight organic acids, such as acetic acid and butyric acid, which lower the pH of the compost [2, 4, 24]. Small fluctuations in pH occur during the compost humification period but maintained at a certain level due to the biosynthesis of humus which act as pH buffer [4]. The pH of the final compost product was ranging from 6.7 to 9.0 indicating that the compost had been decomposed [23, 24].

3.2 UV–visible spectroscopy of DOM

According to Albrecht's study, a class of shoulder peaks appearing at 280 nm in the UV–visible spectrum is the absorption of UV light by conjugated structures in humic substances and aromatic substances present in DOM causing electron π-π* leap, and the UV–visible absorption intensity of humic substances increases as the unsaturated conjugated double bond structure of humic substances and aromatic substances increases [18, 35]. It can be seen that the UV–visible absorption intensity of DOM shows a gentle and gradual decrease with an increase in wavelength indicating that DOM contains humus-like substances and the aromaticity, unsaturation, and degree of humification of humus substances gradually increase with the composting process (Fig. 1) [31, 36].
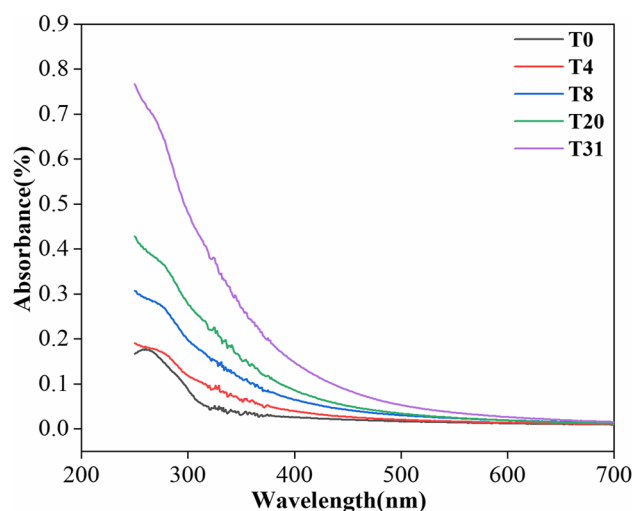

Fig. 1 UV–Vis spectra of DOM samples at different times

Table 2 UV–Visible spectral index of DOM samples at different times

Sample	SUVA$_{254}$	SUVA$_{280}$	E$_{250}$/E$_{365}$	S$_R$
0 d	0.86	0.71	5.00	3.05
4 d	0.93	0.82	3.39	1.42
8 d	1.50	1.31	3.12	1.18
20 d	2.06	1.78	3.16	0.95
31 d	3.73	3.12	3.35	1.08

In order to gain more insight into the chemical composition and change of DOM from UV–visible spectra, several representative parameters SUVA$_{254}$, SUVA$_{280}$, E$_{250}$/E$_{365}$, and S$_R$ were calculated [26, 37]. The initial value of SUVA$_{254}$ and SUVA$_{280}$ was 0.86 and 0.71 which reached their maximum value of about 3.73 and 3.12 at the end of composting (Table 2, indicating the incomplete degradation of condensed amino acids and increased lignin content in the pile; the non-humic substances in the pile were continuously transformed into humic substances during the composting process, and the organic matter with large molecular weight in DOM increased, the humification of the pile deepened, and the aromatization of humic substances increased [38, 39]. E$_{250}$/E$_{365}$ and S$_R$ were 5.00 and 3.05 at the beginning of composting and decreased to 3.35 and 1.08 at the end of composting. The decrease of E$_{250}$/E$_{365}$ indicated that the molecular weight of organic matter and the degree of humification in DOM increased with the deepening of composting [40]. The decrease in S$_R$ with composting is because a large number of small molecules in the pile are degraded and converted into large molecules by microbial degradation and aggregation along with compost humification [26].

3.3 Fourier transforms infrared spectroscopy of DOM

The composition and structure analysis of functional groups of organic compounds in composting are often determined by the wavelengths of specific absorption peaks in FTIR [23, 37]. Different days DOM sample showed absorption peaks at 2930 cm^{-1}, 1645 cm^{-1}, 1400 cm^{-1}, 1103 cm^{-1}, 1000 cm^{-1}, 760 cm^{-1}, and 620 cm^{-1} (Fig. 2). The peak at 2930 cm^{-1} is ascribed to the stretching of C-H, CH$_2$, and CH$_3$ groups in aliphatic and carbohydrates group within the stack [5, 41–43]. Peak at 2930 cm^{-1} is weak at the initial stage of composting indicating that fatty substances and carbohydrates were continuously consumed as the composting progressed. Meanwhile, the peak at 1645 cm^{-1} was weakened which corresponds to the C=C and C=O stretching vibrations of the aromatic components in the amide group and the benzene ring structure in lignin, suggesting that lignin is consumed within the pile as the composting progress [36]. The peak at 1400 cm^{-1} is ascribed to C=N stretching in amides or COO stretching in carboxylic acids [9, 43]. Peak at 1103 cm^{-1} corresponds to the C-O tensile properties of secondary alcohols, ethers, and polysaccharides [5, 43, 44]. Furthermore, the band appear at 1000 cm^{-1} is associated with the carbon–oxygen stretching of the main polysaccharide compounds in the pile, and the comparison before and after composting showed that the wave signal weaken which indicates the consumption of main polysaccharide compounds [45]. Peak at 760 cm^{-1} is ascribed to the wobble vibration of CH$_2$ in cellulose [45], while the band at 620 cm^{-1} is ascribed to the bending bands of N–H and amino compounds within the stack.

Different peaks in FTIR spectrum express useful information about the DOM [43]. As shown in Table 3, peak
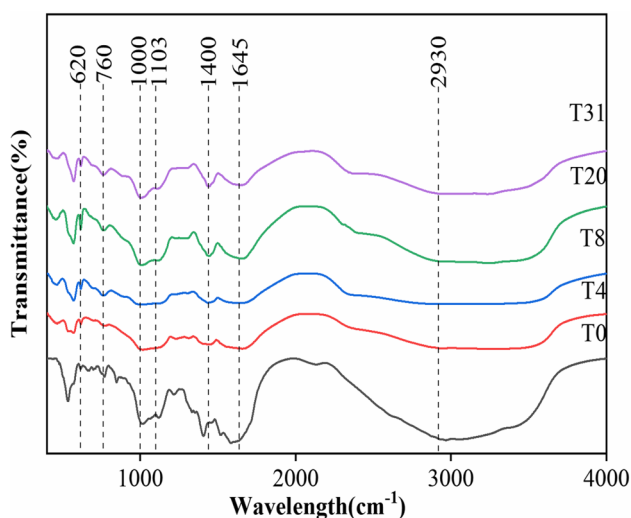
Table 3 The peak intensity ratio of DOM samples at different times

Composting duration (day)	Absorbance ratio at specific wavenumber		
	1645/1103	1645/1400	1645/2930
0 d	0.37	0.73	1.00
4 d	0.72	0.29	0.86
8 d	1.66	0.31	5.30
20 d	1.27	0.43	1.62
31 d	1.32	0.61	2.76

at 1645 cm^{-1}/1103 cm^{-1} (aromatic carbon/alcohol carbon) reached its peak on the 8th day of composting showing an overall increasing trend. The increase in this ratio may be due to the rapid degradation of alcohols and ethers within the compost pile in the early stages and the decomposition of some aromatic structures in the later stages [43, 45]. Peak at 1645 cm^{-1}/1400 cm^{-1} (aromatic C/carboxyl C) decreases in the initial stage following the gradual increases during composting; this fluctuation is due to the organic waste decomposition and oxygen reaction in pile for carboxy C conversion, which latterly expressed the discharge of CO$_2$ [23, 43]. Peak at 1645 cm^{-1}/2930 cm^{-1} (aromatic C/aliphatic C) increased in comparison with an initial stage of composting which might be due to the enhanced activity of microorganisms and rapid organic matter degradation of aliphatic structure in DOM [45].

3.4 Fluorescence spectroscopy of DOM

The fluorescence EEM spectra of DOM at different composting time intervals are shown in (Fig. 3). According to Yu et al. [9, 16], the EEM spectra are generally divided into five different regions (Fig. 3). In the initial stage of composting (0 days), a clear fluorescence peak appears in region IV: peak A (Ex/Em = 275/340) which is associated with soluble microbial by-products [9, 16]. Finding suggests that some biodegradable substances in the compost pile were rapidly decomposed by microorganisms at the early stage of composting, and the growth and metabolic activities were vigorous. From the 4th day, the fluorescence intensity of the peak A decreased continuously which was due to the exhaustion of easily biodegradable substances, the gradual decrease of microbial activity, and the decrease of soluble by-products [27, 42]. From the 4th day to 31st day, a new fluorescence C-peak appeared in the five regions: (Ex/Em = 348/428 nm), which is associated with humic-like substances, and the fluorescence C-peak increases initially and then gradually decreases. The increase in C-peak was due to the continuous production of fulvic acid and humus-like substances within the pile along with composting process which increases the molecular weight and also improves the chemical stability of pile [42, 43]. Fulvic acid and humus-like substances

Fig. 2 FTIR spectra of DOM samples at different times

Fig. 3 Fluorescence excitation-emission matrix spectra of DOM samples at different times
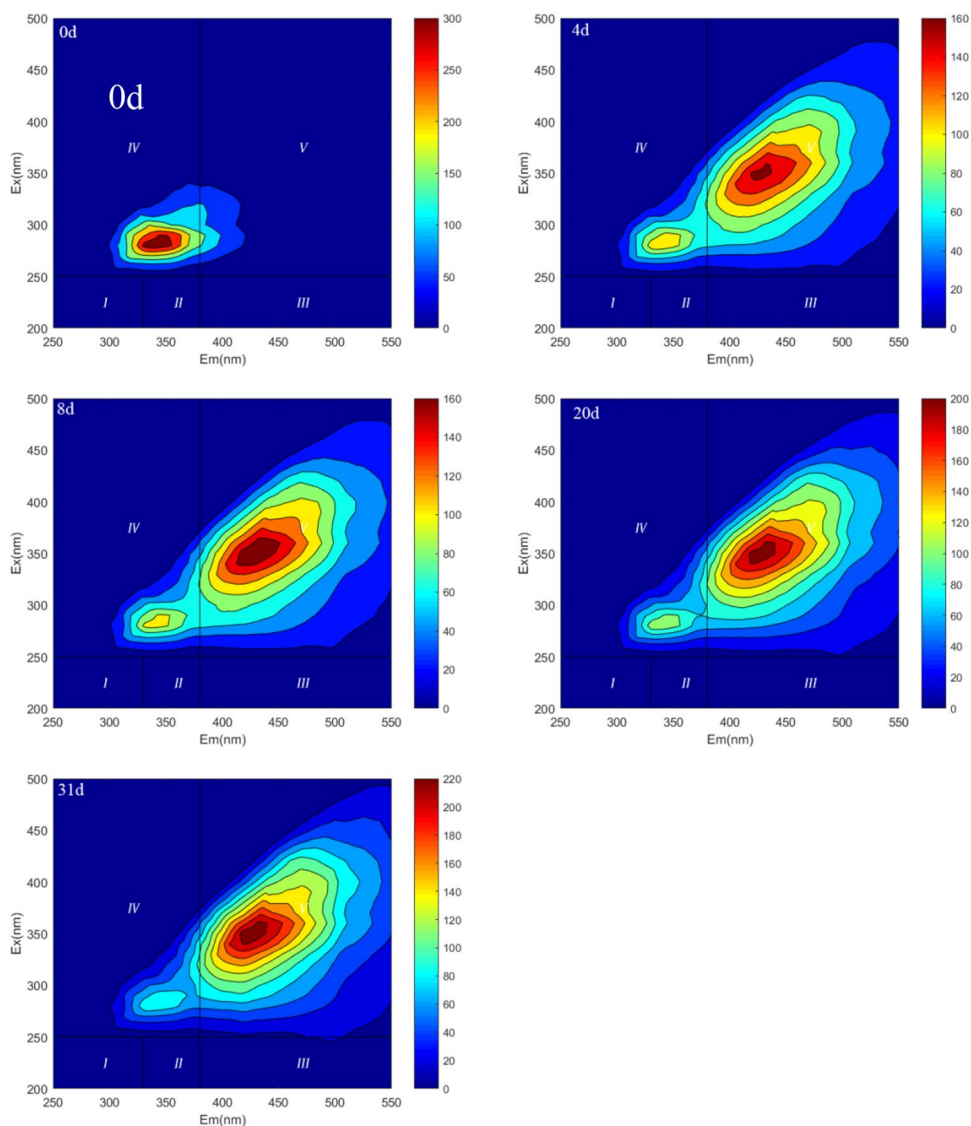

were stable relative to protein-like substances, but they were decomposed and converted to higher levels of stable structures and insoluble humic substances in the later stages of composting which could be a reason behind the decrease in C-peak fluorescence intensity from the 20th day to the 31st day [28, 42].

More information on the characterization of DOM can be obtained by EEM-PARAFAC [44]. In this study, four different components (Ex/Em = 350/435 nm (Component 1, C1), 280/340 nm (Component 2, C2), (250,410)/490 nm (Component 3, C3), and 330/390 (Component 4, C4)) were obtained by EEM-PARAFAC. C1 and C3 represent humic substances, while C2 represents proteins (including tyrosine and tryptophan), and C4 represents xanthohumic acid-like components [17, 24]. The maximum fluorescence intensity (Fmax) of the DOM samples at different composting times is shown in Fig. 4a. While C2 representing protein decreased, humus and

C1, C3, and C4 representing fulvic acid tended to increase, indicating that protein substances (tyrosine, tryptophan, etc.) were easily absorbed as composting progressed [46].

Fluorescence area integral (FRI) is often used to calculate the fluorescence area of the EEM spectrum of a sample [47]. The fluorescence area integration rates $((P_{i,n})\ (_{i=I, II, III, IV, V}))$ shows that $P_{I, n}$ and $P_{II, n}$ are associated with the presence of structurally simple aromatic proteins (tyrosine and tryptophan) as presented in Fig. 4b [35]. $P_{III, n}$ is associated with fulvic acid-like substances [48], while $P_{IV, n}$ is generally considered to be soluble microbial by-product-like substances [23], and $P_{V, n}$ is a complex molecular structure of humic substances [44]. As composting progress, humus-like substances with complex molecular structures were increased, while protein-like substances and soluble microbial by-products were declined [47]. $P_{V, n}/P_{III, n}$ is usually used to characterize the maturity of compost [35]. $P_{V, n}/P_{III, n}$ increased

Fig. 4 **a** Distribution of the four PARAFAC-derived components of DOM samples at different times. **b** Fluorescence area integration of DOM samples at different times
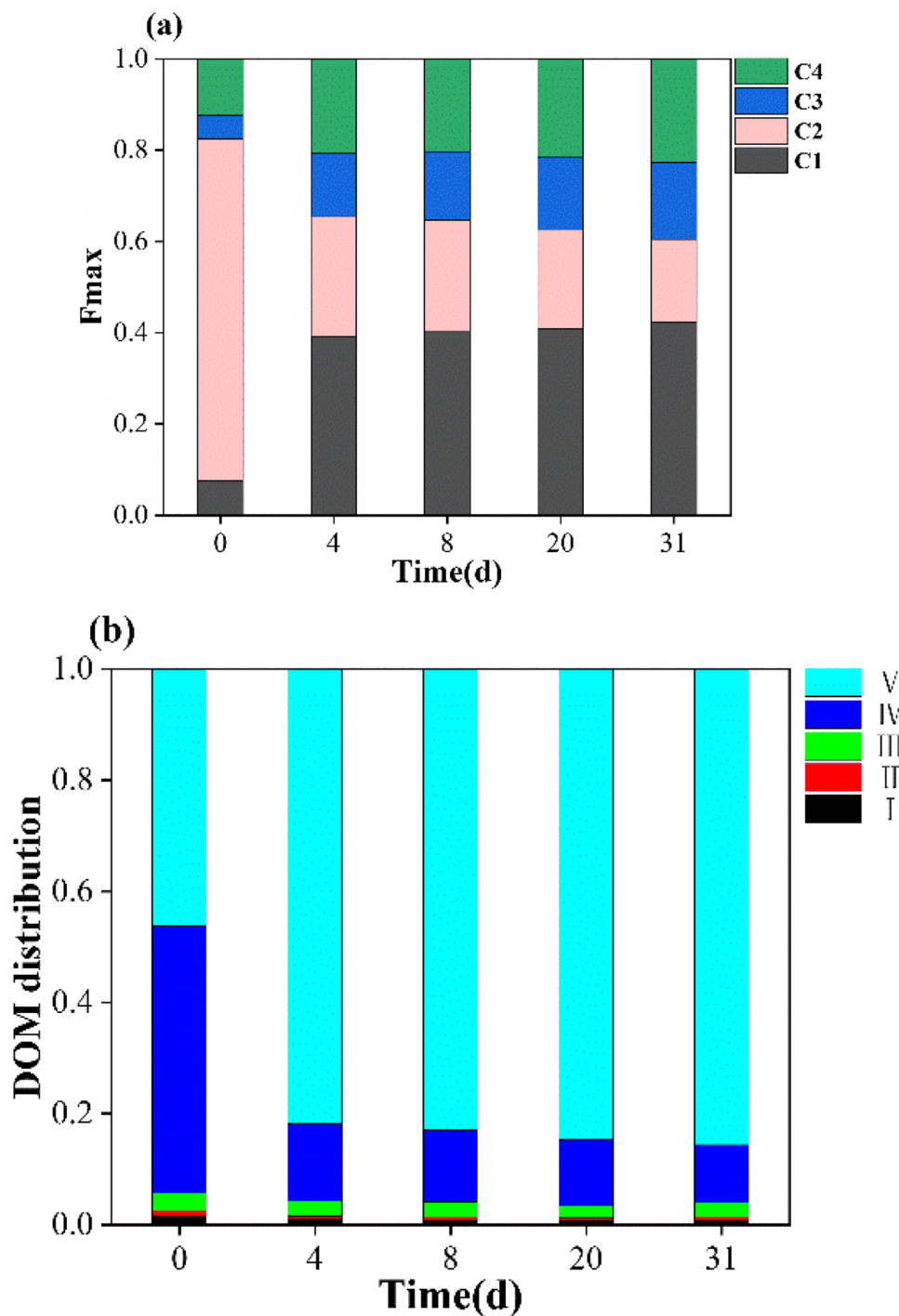
continuously and reached the highest level on the 20th day, but the ratio decreased on the 31st day which may be due to the fact that biodegradable substances had been decomposed completely at the end of composting and microorganisms in the pile could only decompose humus as nutrients.

Fluorescence index (FI) represents the proportion of aromatic amino acids to non-aromatic amino acids in the fluorescence intensity of DOM and can be used to assess

the source of DOM [49, 50]. Table 4 shows that the FI of DOM is more than 1.6 on different days, indicating that the source of DOM in the heap is mainly due to microorganisms in the sludge and there is no exogenous influence [27, 51]. HIX is an important indicator for characterizing the degree of DOM humification ranging from 0 to 1, as the value increases the degree of DOM humification and the strength of aromaticity was also increased [50]. HIX increased from

Table 4 Fluorescence parameters of DOM samples at different times

Time (day)	FI	BIX	HIX	$P_{v,n}/P_{III,n}$
0 d	1.75	2.47	0.14	14.77
4 d	1.86	0.75	0.39	29.56
8 d	1.90	0.77	0.43	31.68
20 d	1.83	0.73	0.55	36.97
31 d	1.87	0.73	0.62	33.33

0.14 (0th day) to 0.62 (31st day) indicating that as composting progressed, protein-like substances were degraded by microorganisms, the content of aromatic-based substances increased, the degree of humification deepened, and the compost gradually reached a stable state [20, 27]. BIX was used to characterize the bioavailability of DOM and was positively correlated with the degree of humification [20]. When the value of BIX is between 0.6 and 0.8, it means that there are fewer internal sources and more external sources of DOM. When the value is between 0.8 and 1.0, it means that the sources of DOM are between internal and external sources, while when the value is greater than 1, it means that DOM is mainly internal sources [52]. BIX value decreases with the composting process and remains around 0.73 in the later stages of composting, indicating that DOM within the pile is strongly influenced by land sources as mentioned in Table 4. Another study showed that BIX can reflect the protein-like substance content of DOM, and larger the BIX, the greater the contribution of protein-like fraction [53], and this result could be mutually proved with EEM-PARAFAC.

3.5 Correlation analysis

Temperature, moisture content, and pH are the basic physicochemical parameters for evaluating the composting process and determining the degree of compost humification [23, 33, 37]. pH and temperature were significantly and positively correlated with water content ($R=0.879$, $p=0.050$; $R=0.940$, $p=0.017$), which indicates that the underlying physicochemical properties can be used to assess the degree of compost maturity (Fig. 5). $SUVA_{280}$ showed a highly significant positive correlation with SUV_{A254} ($R=1.000$, $p=0.000$), indicating that the degree of humification and aromaticity of DOM in the pile increased as the composting proceeded. $SUVA_{254}$ showed a significant negative correlation with $SUVA_{280}$ and water content ($R=-0.916$, $p=0.029$; $R=-0.928$, $p=0.023$), HIX and water content exhibited a highly significant negative correlation ($R=-0.962$, $p=0.009$) because microbial activity in aerobic composting of sludge requires suitable moisture, and a decrease in water content decreases microbial activity and slows down the humification process. The decrease in water content leads toward reduction in microbial activity
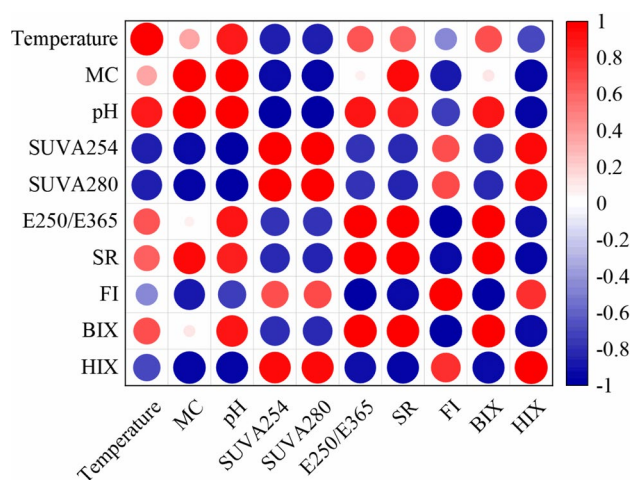
Fig. 5 Correlation of different parameters of compost DOM

and humification process. E_{250}/E_{365} and S_R showed a highly significant positive correlation ($R=0.986$, $p=0.002$) which indicates that with the deepening of humification process, small molecular organic matter decomposes and polymerizes into large molecular organic matter, and the humification degree of DOM is further deepened. BIX and E_{250}/E_{365} were highly significantly and positively correlated with S_R ($R=0.988$, $p=0.02$; $R=0.982$, $p=0.03$) which indicates that BIX can be used to analyze the humification degree in compost.

4 Conclusions

In large-scale industrial sludge composting, combined with basic physical and chemical parameters and a variety of spectral techniques, the maturity of compost can be well evaluated, and safe and healthy mature products can be obtained. The results showed that (1) the duration of the compost > 50℃ and the pH in the range of 6.7–9.0 indicated that the compost was mature, which was confirmed by subsequent spectroscopic analysis; (2) the results of FTIR and EEM spectra show that the decomposition of different substances in the pile can be seen by infrared spectra, as evidenced by three different absorption ratios, while the EEM spectra reflect the conversion of easily decomposed substances into fulvic acid and humic-like substances in the pile; and (3) fluorescence spectroscopy parallel factor (EEM-PARAFAC) analysis proved the conversion of protein material fraction to humus-like material fraction. In this paper, it evaluates the maturity of industrial composting of sludge, but the subsequent determination of nitrogen, phosphorus, and potassium content and heavy metal content of compost products is not carried out, and the subsequent agricultural application of sludge is still a huge challenge.

Data availability The data will be provided on request to the corresponding author.

Declarations

Ethics approval The study does not involve any human or animal subject study.

Consent to participate All authors reviewed and approved the final manuscript.

Consent for publication All authors approved this for publication.

Conflict of interests The authors declare no competing interests.

References

1. Mo Z, Shi Q, Zeng H, Lu Z, Bi J, Zhang H, Rinklebe J, Lima EC, Rashid A, Shahab A (2021) Efficient removal of Cd (II) from aqueous environment by potassium permanganate-modified eucalyptus biochar. Biomass Convers and Biorefin 1–13. https://doi.org/10.1007/s13399-021-02079-4

2. Wang Z, Wu D, Lin Y, Wang X (2022) Role of temperature in sludge composting and hyperthermophilic systems: a review. BioEnergy Res 15:962–976. https://doi.org/10.1007/s12155-021-10281-5

3. Abbasi F, Mokhtari M, Jalili M (2019) The impact of agricultural and green waste treatments on compost quality of dewatered sludge. Environ Sci Pollut Res 26:35757–35766

4. El Fels L, Zamama M, El Asli A, Hafidi M (2014) Assessment of biotransformation of organic matter during co-composting of sewage sludge-lignocelullosic waste by chemical, FTIR analyses, and phytotoxicity tests. Int Biodeterior Biodegradation 87:128–137

5. Asses N, Farhat A, Cherif S, Hamdi M, Bouallagui H (2018) Comparative study of sewage sludge co-composting with olive mill wastes or green residues: process monitoring and agriculture value of the resulting composts. Process Saf Environ Prot 114:25–35

6. Kulikowska D, Sindrewicz S (2018) Effect of barley straw and coniferous bark on humification process during sewage sludge composting. Waste Manage 79:207–213

7. Naserian ES, Cheraghi M, Lorestani B, Sobhanardakani S, Sadr MK (2021) Qualitative investigation of sewage sludge composting: effect of aerobic/anaerobic pretreatments. Arab J Geosci 14:836

8. Xiong R, Gao X, Tu X, Mao Y, Jiang L, Zheng L, Du Y (2022) Heavy metal remediation in sludge compost: recent progress. J Renew Mater 10:469–486

9. Zhang D, Xu Z, Wang G, Huda N, Li G, Luo W (2020) Insights into characteristics of organic matter during co-biodrying of sewage sludge and kitchen waste under different aeration intensities. Environ Technol Innov 20:101117

10. Fan S, Li A, ter Heijne A, Buisman CJN, Chen W-S (2021) Heat potential, generation, recovery and utilization from composting: a review. Resour Conserv Recycl 175:105850

11. Liu X, Hou Y, Li Z, Yu Z, Tang J, Wang Y, Zhou S (2020) Hyperthermophilic composting of sewage sludge accelerates humic acid formation: Elemental and spectroscopic evidence. Waste Manage 103:342–351

12. Nguyen T-B, Shima K (2019) Composting of sewage sludge with a simple aeration method and its utilization as a soil fertilizer. Environ Manage 63:455–465

13. Meng L, Zhang S, Gong H, Zhang X, Wu C, Li W (2018) Improving sewage sludge composting by addition of spent mushroom substrate and sucrose. Biores Technol 253:197–203

14. Zhao X-L, Li B-Q, Ni J-P, Xie D-T (2016) Effect of four crop straws on transformation of organic matter during sewage sludge composting. J Integr Agric 15:232–240

15. Ullah H, Lun L, Riaz L, Naseem F, Shahab A, Rashid A (2021) Physicochemical characteristics and thermal degradation behavior of dry and wet torrefied orange peel obtained by dry/wet torrefaction. Biomass Convers Biorefin. https://doi.org/10.1007/s13399-021-01777-3

16. Yu Z, Liu X, Zhao M, Zhao W, Liu J, Tang J, Liao H, Chen Z, Zhou S (2019) Hyperthermophilic composting accelerates the humification process of sewage sludge: molecular characterization of dissolved organic matter using EEM–PARAFAC and two-dimensional correlation spectroscopy. Biores Technol 274:198–206

17. Huang W, Li Y, Liu X, Wang W, Wen P, Yu Z, Zhou S (2021) Linking the electron transfer capacity with the compositional characteristics of dissolved organic matter during hyperthermophilic composting. Sci Total Environ 755:142687

18. Albrecht R, Le Petit J, Terrom G, Périssol C (2011) Comparison between UV spectroscopy and nirs to assess humification process during sewage sludge and green wastes co-composting. Biores Technol 102:4495–4500

19. He X-S, Xi B-D, Li X, Pan H-W, An D, Bai S-G, Li D, Cui D-Y (2013) Fluorescence excitation–emission matrix spectra coupled with parallel factor and regional integration analysis to characterize organic matter humification. Chemosphere 93:2208–2215

20. Liu J, Liang J, Bravo AG, Wei S, Yang C, Wang D, Jiang T (2021) Anaerobic and aerobic biodegradation of soil-extracted dissolved organic matter from the water-level-fluctuation zone of the Three Gorges Reservoir region. China Sci Total Environ 764:142857

21. Liu M, Tan Y, Fang K, Chen C, Tang Z, Liu X, Yu Z (2021) Diverse molecular compositions of dissolved organic matter derived from different composts using ESI FT-ICR MS. J Environ Sci 99:80–89

22. Zhu Q, Li G, Jiang Z, Li M, Ma C, Li X, Li Q (2020) Investigating the variation of dissolved organic matters and the evolution of autotrophic microbial community in composting with organic and inorganic carbon sources. Bioresour Technol 304:123013. https://doi.org/10.1016/j.biortech.2020.123013

23. Yang Y, Du W, Cui Z, Zhao T, Wang X, Lv J (2020) Spectroscopic characteristics of dissolved organic matter during pig manure composting with bean dregs and biochar amendments. Microchem J 158:105226

24. Abid W, Mahmoud IB, Masmoudi S, Triki MA, Mounier, Amma E (2020) Physico-chemical and spectroscopic quality assessment of compost from date palm (Phoenix dactylifera L.) waste valorization. J Environ Manage 264, 110492

25. Abaker MG, Raynaud M, Théraulaz F, Prudent P, Redon R, Domeizel M, Martino C, Mounier S (2020) Rapid on site assessment of a compost chemical stability parameter by UV and

fluorescence spectroscopy coupled with mathematical treatment. Waste Manage 113:413–421

26. Li P, Hur J (2017) Utilization of UV-Vis spectroscopy and related data analyses for dissolved organic matter (DOM) studies: a review. 1⊠ Crit Rev Environ Sci Technol 47, 131–154.

27. Yan L, Liu C, Zhang Y, Liu S, Zhang Y (2021) Effects of C/N ratio variation in swine biogas slurry on soil dissolved organic matter: content and fluorescence characteristics. Ecotoxicol Environ Saf 209:111804

28. He X, Xi B, Wei Z, Guo X, Li M, An D, Liu H (2011) Spectroscopic characterization of water extractable organic matter during composting of municipal solid waste. Chemosphere 82:541–548

29. Yu G-H, He P-J, Shao L-M (2010) Novel insights into sludge dewaterability by fluorescence excitation–emission matrix combined with parallel factor analysis. Water Res 44:797–806

30. Cui H-Y, Zhao Y, Chen Y-N, Zhang X, Wang X-Q, Lu Q, Jia L-M, Wei Z-M (2017) Assessment of phytotoxicity grade during composting based on EEM/PARAFAC combined with projection pursuit regression. J Hazard Mater 326:10–17

31. Wang X, Chen T, Zheng G (2020) Perlite as the partial substitute for organic bulking agent during sewage sludge composting. Environ Geochem Health 42:1517–1529. https://doi.org/10.1007/s10653-019-00353-z

32. Tang Z, Yu G, Liu D, Xu D, Shen Q (2011) Different analysis techniques for fluorescence excitation–emission matrix spectroscopy to assess compost maturity. Chemosphere 82:1202–1208

33. Xu Z, Li G, Huda N, Zhang B, Wang M, Luo W (2020) Effects of moisture and carbon/nitrogen ratio on gaseous emissions and maturity during direct composting of cornstalks used for filtration of anaerobically digested manure centrate. Biores Technol 298:122503

34. Mandpe A, Tyagi L, Paliya S, Chaudhry S, Motghare A, Kumar S (2021) Rapid-in-house composting of organic solid wastes with fly ash supplementation: performance evaluation at thermophilic exposures. Biores Technol 337:125386

35. Wei Z, Zhao X, Zhu C, Xi B, Zhao Y, Yu X (2014) Assessment of humification degree of dissolved organic matter from different composts using fluorescence spectroscopy technology. Chemosphere 95:261–267

36. Song C, Li M, Xi B, Wei Z, Zhao Y, Jia X, Qi H, Zhu C (2015) Characterisation of dissolved organic matter extracted from the bio-oxidative phase of co-composting of biogas residues and livestock manure using spectroscopic techniques. Int Biodeterior Biodegradation 103:38–50

37. Ren X, Wang Q, Li R, Chang CC, Pan J, Zhang Z (2020) Effect of clay on greenhouse gas emissions and humification during pig manure composting as supported by spectroscopic evidence. Sci Total Environ 737:139712. https://doi.org/10.1016/j.scitotenv.2020.139712

38. Bhat SA, Singh J, Vig AP (2017) Instrumental characterization of organic wastes for evaluation of vermicompost maturity. J Anal Sci Technol 8:2

39. Hagemann N, Subdiaga E, Orsetti S, de la Rosa JM, Knicker H, Schmidt H-P, Kappler A, Behrens S (2018) Effect of biochar amendment on compost organic matter composition following aerobic composting of manure. Sci Total Environ 613–614:20–29

40. Wang L, Wu F, Zhang R, Li W, Liao H (2009) Characterization of dissolved organic matter fractions from Lake Hongfeng, Southwestern China Plateau. J Environ Sci 21:581–588

41. Boukir A, Fellak S, Doumenq P (2019) Structural characterization of Argania spinosa Moroccan wooden artifacts during natural

degradation progress using infrared spectroscopy (ATR-FTIR) and X-Ray diffraction (XRD). Heliyon 5:e02477

42. Guo X, Li C, Zhu Q, Huang T, Cai Y, Li N, Liu J, Tan X (2018) Characterization of dissolved organic matter from biogas residue composting using spectroscopic techniques. Waste Manage 78:301–309

43. He X-S, Xi B-D, Jiang Y-H, He L-S, Li D, Pan H-W, Bai S-G (2013) Structural transformation study of water-extractable organic matter during the industrial composting of cattle manure. Microchem J 106:160–166

44. Che J, Lin W, Ye J, Liao H, Yu Z, Lin H, Zhou S (2020) Insights into compositional changes of dissolved organic matter during a full-scale vermicomposting of cow dung by combined spectroscopic and electrochemical techniques. Biores Technol 301:122757

45. Wang Q, Awasthi MK, Zhao J, Ren X, Wang M, Li R, Wang Z, Zhang Z (2018) Utilization of medical stone to improve the composition and quality of dissolved organic matter in composted pig manure. J Clean Prod 197:472–478

46. He C, He X, Li J, Luo Y, Li J, Pei Y, Jiang J (2021) The spectral characteristics of biochar-derived dissolved organic matter at different pyrolysis temperatures. J Environ Chem Eng 9:106075

47. Li H, Zhang T, Tsang DCW, Li G (2020) Effects of external additives: biochar, bentonite, phosphate, on co-composting for swine manure and corn straw. Chemosphere 248:125927

48. Wang Q, Awasthi MK, Ren X, Zhao J, Li R, Wang Z, Wang M, Chen H, Zhang Z (2018) Combining biochar, zeolite and wood vinegar for composting of pig manure: the effect on greenhouse gas emission and nitrogen conservation. Waste Manage 74:221–230

49. McKnight DM, Boyer EW, Westerhoff PK, Doran PT, Kulbe T, Andersen DT (2001) Spectrofluorometric characterization of dissolved organic matter for indication of precursor organic material and aromaticity. Limnol Oceanogr 46:38–48

50. Zhang Y, Zhang E, Yin Y, van Dijk MA, Feng L, Shi Z, Liu M, Qina B (2010) Characteristics and sources of chromophoric dissolved organic matter in lakes of the Yungui Plateau, China, differing in trophic state and altitude. Limnol Oceanogr 55:2645–2659

51. Fellman JB, Hood E, Spencer RGM (2010) Fluorescence spectroscopy opens new windows into dissolved organic matter dynamics in freshwater ecosystems: a review. Limnol Oceanogr 55:2452–2462

52. Huguet A, Vacher L, Relexans S, Saubusse S, Froidefond JM, Parlanti E (2009) Properties of fluorescent dissolved organic matter in the Gironde Estuary. Org Geochem 40:706–719

53. Guo X, He X, Zhang H, Deng Y, Chen L, Jiang J (2012) Characterization of dissolved organic matter extracted from fermentation effluent of swine manure slurry using spectroscopic techniques and parallel factor analysis (PARAFAC). Microchem J 102:115–122. https://doi.org/10.1016/j.microc.2011.12.006